Superconducting UPt_3 in a magnetic field

S. K. Sundaram
Department of Physics and Applied Superconductivity Center, University of Wisconsin–Madison, 1150 University Avenue, Madison, Wisconsin 53706

Robert Joynt
Institute for Theoretical Physics, University of California, Santa Barbara, California 93106 and Department of Physics and Applied Superconductivity Center, University of Wisconsin–Madison, 1150 University Avenue, Madison, Wisconsin 53706

(Received 19 May 1989; revised manuscript received 12 July 1989)

We use earlier calculations of the possible phases of UPt_3 in a magnetic field and recent measurements to identify all the anisotropic superconducting phases of UPt_3. We also determine more precisely the structure of the high-field phases and demonstrate their stability by an exact solution of the Ginzburg-Landau equations at the normal-superconducting phase boundary. The upper critical field as a function of temperature shows upward curvature. This is identified as arising from coupling of superconductivity and antiferromagnetism.

I. INTRODUCTION

A number of recent measurements have established the existence of a rich phase diagram for UPt_3 in the field-temperature (H-T) plane. This began with ultrasound measurements of Müller *et al.*,[1] and Qian *et al.*,[2] with a field along the c axis, which showed two separate superconducting phases. Volovik[3] noted that the zero-field phase of a d-wave superconductor might be different from the phase near H_{c2} by finding particular solutions of the Ginzburg-Landau equations. This phase transition was confirmed by torsional oscillator measurements of Kleiman *et al.*[4] Further ultrasound measurements of Schenstrom *et al.*,[5] with H in the basal plane, demonstrated that there was also more than one phase for this case, and that the phase boundary was different. These authors proposed a vortex core transition to explain their data. Joynt[6] did a general variational analysis of the Ginzburg-Landau equations, and determined all possible phases of a d-wave superconductor at high fields, for both orientations. This paper also proposed a phase diagram for UPt_3 in particular, and gave a mechanism which predicted the two zero-field superconducting transitions, subsequently observed in specific-heat experiments by Fisher *et al.*[7] These measurements have now been done at finite fields directed in the basal plane by Hasselbach *et al.*[8] The specific-heat and upper-critical-field experiments have been analyzed by Hess *et al.*,[9] and by Machida and Ozaki,[10] and have been shown to be quantitatively consistent with the phases proposed in Ref. 6.

The purpose of this report is twofold: First, to elaborate on the observed phases for both directions of the field, and second, to demonstrate by an exact solution that there are two high-field phases when the field is along the c axis, a point which is crucial for the overall picture.

We first review the notation and results of Ref. 6. A d-wave (E_{1g}) superconductor with hexagonal crystal symmetry is characterized by a two-dimensional order parameter $\boldsymbol{\psi}=(\psi_x,\psi_y)$. Different phases have different relative values of ψ_x and ψ_y. The free-energy density is given by

$$F=\alpha_0(T-T_c)\boldsymbol{\psi}\cdot\boldsymbol{\psi}^*+\beta_1(\boldsymbol{\psi}\cdot\boldsymbol{\psi}^*)^2+\beta_2|\boldsymbol{\psi}\cdot\boldsymbol{\psi}|^2 + \sum_{ij}(K_1 p_i\psi_j p_i^*\psi_j^*+K_2 p_i\psi_i p_j^*\psi_j^*+K_3 p_i\psi_j p_j^*\psi_i^*) + K_4\sum_i |p_z\psi_i|^2 . \quad (1)$$

Here β_1, β_2, K_1, K_2, K_3, and K_4 are constants and

$$p_x=-i\partial/\partial x+(2e/\hbar c)A_x$$

and similarly for p_y and p_z, where $\mathbf{A}$ is the vector potential. The total free energy can be minimized in the absence of a field, and one finds solutions[11] $\boldsymbol{\psi}=\psi(1,\pm i)$ and $\boldsymbol{\psi}=\psi(1,0)$. These are called the A and C phases, respectively. Either can be rotated in the plane, of course: $\boldsymbol{\psi}=\psi(0,1)$ is still phase C. More difficult, but still exactly soluble at H_{c2}, is the case with a finite field. At H_{c2} with H along the c axis, the stable phases are again the A phase and another more complicated phase in which the ratio of ψ_x and ψ_y is spatially dependent and intrinsically complex. This is called phase U (for "unsymmetric"). The relation of this phase to the B phase of Ref. 6 is discussed below. The precise form of the U phase is given in Sec. III. At H_{c2} with H in the basal plane the C phase is the only stable one. If a small coupling to the antiferromagnetic order parameter $\mathbf{M}_s=M_s\hat{\mathbf{x}}$ (Refs. 12 and 13) is added to F, we get a term[9,10] $b|\mathbf{M}\cdot\boldsymbol{\psi}|^2=bM_s^2|\psi_x|^2$. This splits the phase transition in the zero field into two, if and only if the low-field solution of (1) is the A phase.[14] If the $H=0, T=0$ phase was the C phase then it would be stable at all $T<T_c$. The A phase is also predicted to be stable in zero field by a microscopic calculation,[15] but more work needs to be done to make this result convincing.[16,17] The specific-heat experiments demonstrate that at $H=0$ and $T=0$, UPt_3 is in the A phase.

II. EXPERIMENTAL PHASE DIAGRAM

The phase diagram for H along the c axis is given in Fig. 1, and is taken from Refs. 1 and 7. Reference 2 does not find a line reaching down to the $H=0$ axis, but the specific-heat data show that there must be such a line. We have followed Ref. 1 in joining this line to the $T=0$ axis, and we base our considerations on this picture. Reference 4 also proposes an additional phase, but its existence is still not confirmed. In accord with the above Ginzburg-Landau analysis we identify the phases as shown. The pure C phase occupies only a small portion of the $H=0$ axis and evolves continuously into the U phase as H increases. The A-U transition is most likely first order, terminating in a second-order point. Additional strong support for this phase diagram comes from recent neutron scattering[18] results which determine $M_s(H,T)$. In these experiments, $M_s(T)$ was measured along a line of constant H which crossed both phase boundaries in Fig. 1. As T decreases, M_s^2 first increases linearly as T_N-T, where T_N is the Néel temperature. In the U phase M_s is constant, indicating a probable kink in $M_s(T)$ at the phase boundary. In the A phase, M_s actually begins to decrease. This can be understood as follows. In the U phase, the order parameter is able to rotate freely to minimize the coupling proportional to b, because in this phase $|\psi_x|$ and $|\psi_y|$ are not equal. As we go into the A phase, $|\psi_x|$ and $|\psi_y|$ are constrained to be equal and therefore ψ cannot reorient to minimize the coupling. M_s must decrease instead.

When H is in the basal plane, there must be a phase transition between the C phase at high fields, which is the only phase allowed, to the A phase, which, as we have already seen, is the low-field phase. The phase boundary is observed in the experiments of Ref. 2, which have been collected together with the specific-heat data by Hasselbach *et al.*[8] to get the diagram shown in Fig. 2. Notice that the experiments are not sufficiently sensitive to distinguish the two possibilities shown for the topology of the phase diagram. Hess *et al.*[9] have pointed out that the kink in $H_{c2}(T)$ is due to the fact that above a certain field, the stable C phase is oriented by the applied field, while below that field, the orientation is determined by the coupling to $\mathbf{M}_s$, as we have already seen. $\mathbf{M}_s$ has six equivalent domains, so we expect the direction of ψ to vary through the sample at low fields but to be uniform at very high fields. (This is discussed in detail in Sec. IV.) We therefore christen the two states C_f (for "field aligned") and C_d (for "domain aligned"). It is important to note that there is no true phase transition between these two states, since the microscopic symmetry is not changed. ψ simply reorients in the various domains in a manner which will depend on the history of the sample. So either of the two topologies shown is possible. If C_f and C_d were really thermodynamically distinct, then one would have four phases meeting at a point in the Hasselbach *et al.* proposal. This would contradict the Gibbs rule.

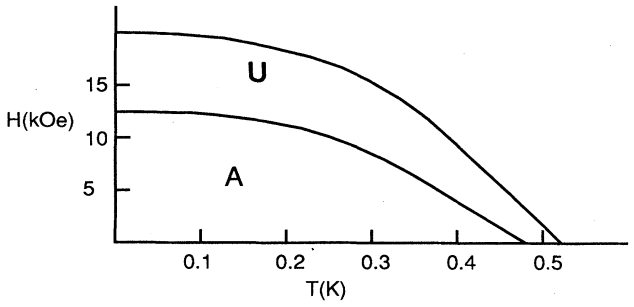

FIG. 1. Phase diagram for UPt_3 when the magnetic field H is along the c axis. The definitions of the phases and their identification are described in the text.

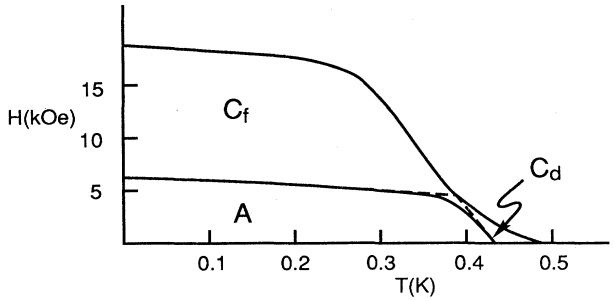

FIG. 2. Phase diagram for UPt_3 when the magnetic field H is in the basal plane. The dashed line indicates the phase boundaries postulated in Ref. 8, which, however, is based on various measurements taken on different samples. The discussion in this paper is based on the simpler diagram given by the solid lines. The definitions of the phases and their identification are described in the text.

The question of what the phases are when H is not along the c axis or in the basal plane is difficult to answer precisely, since the H_{c2} equations appear to have no analytic solution. It seems clear that the C phase can evolve continuously into the B phase as the out-of-plane angle increases. Thus, the point where this angle is zero can be considered as a critical point, since only here is one of the components, ψ_x or ψ_y, exactly equal to zero.

One can see from this analysis that if the Ginzburg-Landau analysis proposed here is accepted as producing the ultrasound and specific-heat anomalies, then the phase diagram of UPt_3 may be regarded as uniquely determined. The vortex-core transition mechanism proposed in Ref. 5 is quite distinct. These authors fix the "background" phase surrounding a vortex core, which can undergo a change of morphology without a change in the background. The present mechanism by contrast is a change in the background. Its weakness is that the equations can only be solved along the $H=0$ and the $H_{c2}(T)$ curves. Thus, no detailed characterization of the transition (its order, for example) can be given.

There is no reason why the two types of transition could not both occur in the same material. For example, if we accept the conclusion[4] from the torsional oscillator data that there is yet another phase boundary dividing region A of Fig. 1 into two parts, then this additional transition could be explained by the vortex-core mechanism.

This would leave the explanation given here of the other phase boundaries intact.

III. THE U PHASE

The U phase is the only one which we have not yet completely defined. It is in some ways the most interesting, since it occurs only at high fields and has no spatially homogeneous analog, as do phases A and C.

It occurs only when H is along the c axis. To find it we need to minimize the quadratic part of $\gamma=\int F\,dx$, taken from Eq. (1). Varying this with respect to ψ_x^* and ψ_y^*, we obtain the equations[9]

$$[(K+K_1)p_x^2+K_1p_y^2]\psi_x+(K_2p_xp_y+K_3p_yp_x)\psi_y = -\alpha_0(T-T_c)\psi_x ,$$
$$(K_2p_yp_x+K_3p_xp_y)\psi_x+[K_1p_x^2+(K+K_1)p_y^2]\psi_y = -\alpha_0(T-T_c)\psi_y , \tag{2}$$

where $K\equiv K_2+K_3$.

In the Hilbert space of ψ, the operation represented by the left-hand side of this equation is Hermitian and has a complete set of eigenfunctions. Finding the lowest eigenvalue of this operator (which is a function of H) determines the upper critical field. The equation is analogous to a Schrödinger equation for a particle in a magnetic field with spin-orbit coupling. It can be solved exactly by the following transformation. Define

$$p_\pm=(l/\sqrt{2})(p_x\pm ip_y)$$

with $l^2=\hbar c/2eH$, so that $[p_-,p_+]=1$. Also let $\psi_\pm=(\psi_x\pm i\psi_y)/\sqrt{2}$. Substitution into Eq. (2) yields

$$[(2K_1+K)(p_+p_-+\tfrac{1}{2})-K'/2]\psi_+ +Kp_+^2\psi_- = -\alpha_0(T-T_c)l^2\psi_+ ,$$
$$Kp_-^2\psi_+ +[(2K_1+K)(p_+p_-+\tfrac{1}{2})+K'/2]\psi_- = -\alpha_0(T-T_c)l^2\psi_- , \tag{3}$$

where $K'=K_2-K_3$.

We now take ψ_+ and ψ_- in the occupation number representation which diagonalizes

$$p_+p_-:\ \psi_+=\sum_0^\infty a_n|n\rangle_+,\quad \psi_-=\sum_0^\infty b_n|n\rangle_- .$$

Then

$$p_+^2|n\rangle=\sqrt{(n+1)(n+2)}\,|n+2\rangle ,$$
$$p_-^2|n\rangle=\sqrt{n(n-1)}\,|n-2\rangle,\quad n\geq 2 ,$$

and $p_-|0\rangle=0$. It is then immediately evident that the problem breaks up into disjoint subspaces spanned by $\{|0\rangle_+\}$, $\{|0\rangle_-,|2\rangle_+\}$, $\{|2\rangle_-,|4\rangle_+\}$, etc. There are also subspaces with odd numbers of quanta, but these can never be the ground state. Only the first two spaces are candidates for the lowest eigenvalue. In fact, $|0\rangle_+$ is the solution first found by Volovik,[3] and is precisely the A phase. In real space it is simply $\psi(\mathbf{r})\cdot(1,-i)$, where $\psi(\mathbf{r})$ is any function belonging to the lowest Landau level. The eigenvalue is $\varepsilon_A=K_1+K_3$ which gives a critical field of

$$H_{c2}=\alpha_0\hbar c(T_c-T)/2e(K_1+K_3) ,$$

in agreement with earlier results. The other possible phase is of the form $\alpha|0\rangle_-+\beta|2\rangle_+$, where α and β are coefficients to be determined. We then find a lowest eigenvalue

$$\varepsilon_B=3K_1+3K/2-\tfrac{1}{2}[(4K_1+2K-K')^2+8K^2]^{1/2} ,$$

and a critical field

$$H_{c2}=\alpha_0\hbar c(T_c-T)/2e\varepsilon_U .$$

For large enough K, we have $\varepsilon_U<\varepsilon_A$, and the U phase has a higher critical field. It is then the stable phase. The stability regions are shown in Fig. 3. The stability diagram is very similar but not identical to that for the earlier variational solution of Ref. 6. (See Fig. 2 of that paper.)

We plot a single "bubble" of the A and U phases in Fig. 4. For this we choose the symmetric gauge $\mathbf{A}=H(-y/2,x/2)$. A simple Gaussian

$$\exp[-(x^2+y^2)/4l^2]$$

belongs to the lowest Landau level, and phase A has just the symmetric appearance of this function for both of its components ψ_x and ψ_y. The supercurrents flow azimuthally and the phase may be thought of as being stable when the coupling of the orbital supercurrent to the field is dominant. The U phase in the same gauge and the same basis is pictured in Fig. 5. One notes immediately that rotational symmetry is broken, so that the supercurrents tend to flow along one axis. This phase is stable when the coupling of the supercurrent to the direction of ψ itself dominates. This sort of coupling is peculiar to anisotropic superconductivity and has no analog in the s-

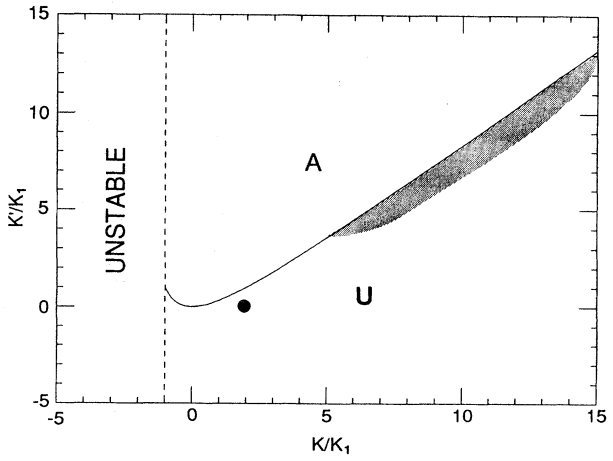

FIG. 3. Region of stability for the A and U phases as a function of the Ginzburg-Landau parameters defined by Eq. (1). In the unstable region, the system's free energy is not bounded below and is therefore not physical. The shaded region is the region which gives a reasonable fit to $H_{c2}(T)$ data. The circle is the weak coupling point.

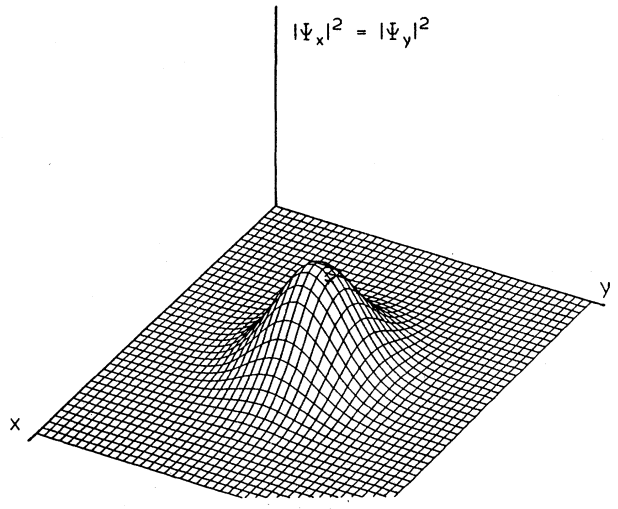

FIG. 4. Shape of a single vortex belonging to the A phase. $|\psi_x|^2=|\psi_y|^2$ is shown.

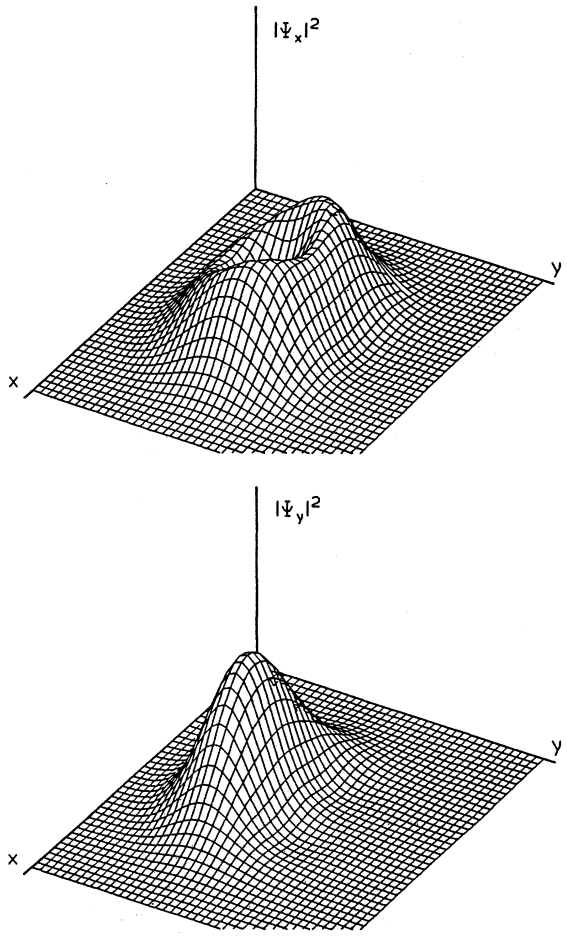

FIG. 5. Shape of a single vortex in the U phase. $|\psi_x|^2\neq|\psi_y|^2$ and rotational symmetry is spontaneously broken.

wave case. It is evident that a change in the symmetry of the vortex lattice can occur during the A-U transition.

There is one interesting difference between phases A and U. Phase A is completely independent of the parameters in the free energy. It has precisely the same form everywhere in region A of Fig. 3. Phase U, on the other hand, has the coefficients α and β in its definition. These are complicated functions of the parameters. This has the important consequence that the U phase may be expected to evolve continuously as H and T change with possible changes in the shape of the unit cell of the vortex lattice, for example, whereas the A phase should maintain a triangular lattice, though perturbed by the coupling to the antiferromagnetism, neglected in Eq. (2).

Furthermore, the U phase breaks rotation symmetry and can reorient itself in the basal plane. This is important when we consider the coupling to M_s, otherwise neglected in this section. The U phase will have a smaller resulting value of the coupling than the A phase because of this additional degree of freedom. Correspondingly, we would expect a smaller value for M_s in the A phase than in the U phase. As we noted above, there is evidence for precisely this effect in neutron scattering experiments which measure $M(H,T)$ across the A-U phase boundary. The exact solution given here for the U phase was found earlier, and independently, by Zhitomirskii.[19]

The exact solution for the U phase is similar to the B phase of Ref. 6 in that the behavior under the point group and time reversal is the same. For both phases at H_{c2}, when the problem is precisely linear, the eigenfunctions of the lowest level cannot be chosen to be invariant under any of the symmetry operations. Thus, for example, a vortex lattice formed below H_{c2} by a linear superposition of the eigenfunctions would break the hexagonal symmetry in both cases. This would not necessarily be the case for the A phase as noted above, allowing either B or U to be distinguished from A in, for example, decoration experiments.

The general issue which this raises, however, is to what extent the precise form of the lowest eigenfunctions allows one to characterize a phase. The eigenfunctions apply, strictly speaking, only at H_{c2}, whereas we wish to unambiguously identify different phases in a finite region of the H-T plane. In fact, the criterion of determining the point-group symmetry is not always sufficient for the simple reason that the nonlinear terms can break down these symmetries, even at an infinitesimally small distance away from H_{c2}. In the isotropic case, for example, axial symmetry breaks down to hexagonal symmetry immediately, because of the formation of the vortex lattice. Indeed, in the full nonlinear regime it seems to be very difficult to formulate a criterion based on the solutions at H_{c2} which would allow different solutions to be distinguished. On the other hand, very near H_{c2} there is a perturbative regime where only linear combinations of the lowest eigenfunctions are allowed. The mathematical problem is to identify properties of this finite-dimensional subspace which differ from one phase to another. This appears difficult, and we do not pursue that issue further in generality. It is important to point out in this special case that the B phase and the U phase could, in principle,

be distinguished on this basis. The chief difference between them is that the ratio of ψ_x and ψ_y is constant in the B phase and spatially varying in the U phase. This difference remains for all linear combinations.

IV. UPPER CRITICAL FIELDS IN THE PRESENCE OF A STAGGERED MAGNETIZATION

So far we have considered the solutions for the A and U phases in the absence of a coupling to the staggered magnetization. However, this coupling can produce changes in the shape of the upper-critical-field curves $H_{c2}(T)$.[9,20]

Let us deal first with the case where $\mathbf{H}$ is directed in the basal plane. Then at H_{c2} we need only consider the C phase $\boldsymbol{\psi}=\psi(1,0)$, and rotations in the plane. This is the only stable phase when the field is in the plane. There is now an important orienting effect because of the coupling term $b|\mathbf{M}_s\cdot\boldsymbol{\psi}|^2$. $\boldsymbol{\psi}$ will be perpendicular to $\mathbf{M}_s$ at the zero applied field if $b>0$, and parallel if $b<0$. But we expect $\hat{\mathbf{M}}_s$ to vary through the system, because there are six equivalent domains. All of these will be equally populated if no attempt is made to align them (by field cooling, for example).

Let us first focus attention on a single domain, as done by Hess *et al.*[9] At a low applied field the coupling to $\mathbf{M}_s$ determines the direction of $\boldsymbol{\psi}$. At a higher field (how high depending on the relative orientation of $\boldsymbol{\psi}$ and $\mathbf{M}_s$) there will be a sudden change in the direction of $\boldsymbol{\psi}$ if $\mathbf{M}_s\perp\mathbf{H}$. This can produce a kink in H_{c2}. If $\mathbf{M}_s$ is at an arbitrary angle to $\mathbf{H}$, then there is a continuous reorientation of $\boldsymbol{\psi}$, as we show below.

Now consider all six domains. Each has the same T_c at $H=0$, but in general each will have a slightly different critical field. Thus, the "H_{c2}" of the sample will depend on the way it is measured. A resistive measure will give the field at which enough domains have gone superconducting that a percolating path has formed in the sample. A magnetization measurement would yield quite a different average of the critical fields of the various domains.

What then, produces the kink observed in some experiments[8,21] but not in others?[20] Presumably the kink occurs in a situation where the field is very close to the magnetization direction (the $b>0$ case) of one of the six domains. When these particular critical domains go superconducting, then the percolating path is set up—so in effect one is measuring the H_{c2} of a subset of domains all having the same $\mathbf{M}_s$. Thus, the theory of Hess *et al.* goes through, and there is a kink. If the field is in an intermediate direction, or if there is even small mosaic spread in the crystal, then there will be upward curvature in H_{c2}, but no kink.

As an illustration of this we take a case where $\mathbf{H}$ is at an angle of 45° to $\mathbf{M}_s$. The calculation of H_{c2} then proceeds as follows. The free energy is

$$\gamma=\int d^3x[\alpha_0(T-T_c)\boldsymbol{\psi}\cdot\boldsymbol{\psi}^*+K|p_y\psi_y|^2 +K_1|p_y\psi_x|^2+K_4(|p_z\psi_x|^2+|p_z\psi_y|^2) +bM_s^2\boldsymbol{\psi}\cdot\boldsymbol{\psi}^*+bM_s^2(\psi_x\psi_y^*+\psi_x^*\psi_y)]\ . \quad (4)$$

Here we have chosen the axes so that $\mathbf{H}=H\hat{\mathbf{x}}$, $\mathbf{A}=-z\hat{\mathbf{y}}$, and $\hat{\mathbf{M}}_s=(1/\sqrt{2},1/\sqrt{2})$. This can be minimized by choosing ψ_x and ψ_y separately to lie in the lowest Landau level and diagonalizing the resulting quadratic form. One then sees that the upper critical field is given implicitly by

$$-\alpha_0(T-T_0)=\frac{eH}{\hbar c}(\sqrt{K_4K_1}+\sqrt{K_4K}\,)+bM_s^2 -\left[\left[\frac{eH}{\hbar c}\right]^2(\sqrt{K_4K_1}-\sqrt{K_4K}\,)^2 +b^2M_s^4\right]^{1/2}. \quad (5)$$

A fit of this equation to the H_{c2} observed in Ref. 20 is given in Fig. 6. These data were also obtained by a resistance measurement in which it was found that H_{c2} was independent of the direction of H in the basal plane. We took 45° as a reasonable average angle between $\mathbf{H}$ and $\mathbf{M}_s$, rather than attempting to average over domains. In the absence of detailed knowledge of the domain structure and the criteria used to define H_{c2}, the latter procedure is not well defined. The 45° curve gives a perfectly adequate fit to the observed results.

Now let us turn to the situation with $\mathbf{H}$ along the c axis. The angle between $\mathbf{H}$ and $\mathbf{M}_s$ is always 90° because $\mathbf{M}_s$ always lies in the basal plane. Thus, all domains are equivalent. We consider two different phases A and U, although it does not appear that the A phase is ever realized at high fields in UPt_3.

Take phase A first. We rewrite the coupling $bM_s^2|\psi_x|^2$ as $bM_s^2(\psi_+\psi_-^*+\psi_+^*\psi_-)$. The A phase is the phase where the coupling of ψ_+ to ψ_- from the gradient terms, proportional to K, is small (see Sec. III). Thus, unless we are very close to the A-U boundary, we obtain a good approximation to the solution by considering only the subspace $\{|0\rangle_+,|0\rangle_-\}$, with the two states coupled only by the b parameter. Thus the variational equations become

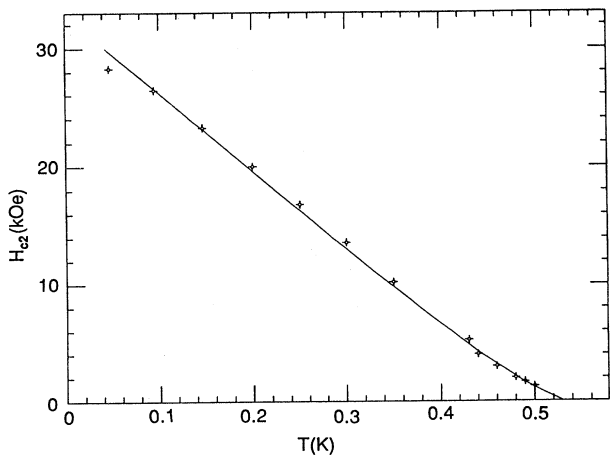

FIG. 6. $H_{c2}(T)$ for $\mathbf{H}$ in the basal plane, experimental data (points) from Ref. 20. The theoretical curve (line) is taken from Eq. (5).

$$[l^2bM_s^2+(K_1+K_3)]\psi_+ + il^2bM_s^2\psi_- = -\alpha_0(T-T_c)l^2\psi_+ ,$$

$$-il^2bM_s^2\psi_+ + [(K_1+K_2)+l^2bM_s^2]\psi_- = -\alpha_0(T-T_c)l^2\psi_- .$$

The lowest eigenvalue is

$$\frac{eH}{\hbar c}[(2K_1+K_2+K_3)+bM_s^2] - \left[\left[\frac{eH}{\hbar c}(K_3-K_2)\right]^2 + b^2M_s^4\right]^{1/2} ,$$

and the critical field is given by setting this equal to $-\alpha(T-T_c)$. This means that $H_{c2}(T)$ shows upward curvature, with

$$-dH_{c2}/dT|_{T_c} = \alpha_0\hbar c/e(K+K_1) ,$$

and

$$-dH_{c2}/dT \rightarrow \alpha_0\hbar c/e(K+K_1-|K_2-K_3|) ,$$

when

$$H \gg \hbar cbM_s^2/e|K_2-K_3| .$$

This means that $H_{c2}(T)$ can appear linear, as observed experimentally, only if $K_2 \approx K_3$, or more precisely if $|K_2-K_3| \ll K+K_1$. As noted by Tokuyasu *et al.*,[22] $K_1=K_2=K_3$ in weak coupling theory.

In the U phase, the whole problem becomes much more complicated. All the blocks of the Hamiltonian are coupled by the b term, and it is no longer possible to find the lowest eigenvalue analytically. However, since the eigenfunctions belonging to the lowest eigenvalues are well localized in the lowest few Landau levels, it is a very good approximation for these levels to truncate the Hamiltonian matrix in the occupation number space. The eigenvalues and eigenvectors can then be calculated numerically, and from this the upper critical field can be obtained. We have done this and find that if K/K_1 is not too large ($\lesssim 15$), then there is not very much curvature in the upper critical field, as observed. A good fit was obtained by choosing $\hbar c\alpha_0/eK_1=25T/K$, $K/K_1=7$, and $K'/K_1=5.4$. The H_{c2} curve obtained in this way is compared to the data of Ref. 23 in Fig. 7. To be consistent with the experimental data, we find that the K parameters must lie in the shaded region of Fig. 3. Thus, the experiments put very important constraints on the parameters in the Landau free energy, which, in turn, gives clues for the microscopic theory. The conclusion at the present time is that weak coupling is not a terribly good approximation for UPt_3. It does give the correct phase at all fields, however, which is unlike the situation for the A phase of ^{3}He.

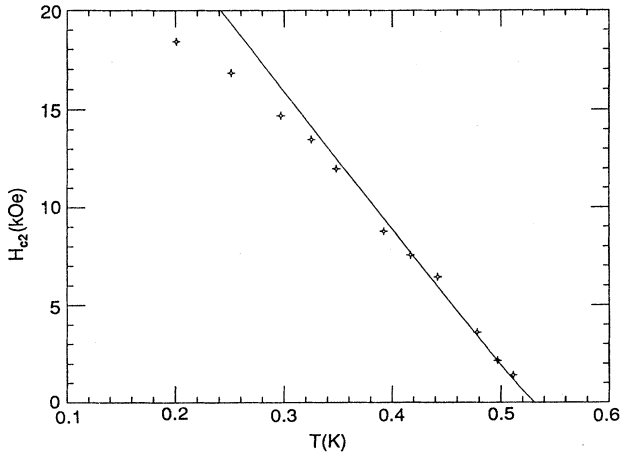

FIG. 7. $H_{c2}(T)$ for **H** along the c axis, data from Ref. 21. The theoretical curve is obtained numerically, with the assumption that the system is in the U phase at H_{c2}.

V. CONCLUSION

We have presented the Ginzburg-Landau theory of superconductivity in UPt_3 regarding this system as a d-wave superconductor belonging to the representation E_{1g}. The chief result is that the phases observed in the H-T plane can be identified from this analysis, which is based on symmetry alone. UPt_3 has three distinct superconducting phases: the A phase which is realized at low temperatures and fields; the U phase which is only realized at high fields and only when the field is along the c axis; and finally the C phase which occurs at high transverse fields and in a small region of temperature at zero field, where the antiferromagnetic moment acts effectively as a transverse field. This identification allows us to understand precisely what change of symmetry is taking place at each peak in the ultrasound and specific-heat experiments. It also gives a good account of the change in the antiferromagnetic moment at these phase boundaries as this change is observed in neutron scattering experiments.

The shape of critical-field curves is strongly affected by the coupling of superconductivity and antiferromagnetism. In particular, $H_{c2}(T)$ shows upward curvature experimentally when the applied field is in the basal plane. This is nicely explained by the Ginzburg-Landau theory. UPt_3 shares this feature with URu_2Si_2. The parameters which one obtains from fitting the H_{c2} curves suggest that there are deviations from the weak coupling theory, though this theory gives a reasonable picture of the overall phase diagram.

ACKNOWLEDGMENTS

We would like to thank G. Crabtree, J. A. Sauls, D. Hess, and T. Tokuyasu for useful discussions. The research was supported by the Electric Power Research Institute and by the National Science Foundation under Grant Nos. DMR-8812852 and PHY82-17853, supplemented by funds from the National Aeronautics and Space Administration.

[1]V. Müller, C. Roth, D. Maurer, E. Scheidt, K. Lüders, E. Bucher, and H. Bommel, Phys. Rev. Lett. **58**, 1224 (1987).
[2]Y. J. Qian, M.-F. Xu, A. Schenstrom, H.-P. Baum, J. B. Ketterson, D. Hinks, M. Levy, and B. K. Sarma, Solid State Commun. **63**, 599 (1987).
[3]G. E. Volovik, J. Phys. C **21**, L221 (1988).
[4]R. N. Kleiman, P. L. Gammel, E. Bucher, and D. J. Bishop, Phys. Rev. Lett. **62**, 328 (1989).
[5]A. Schenstrom, M.-F. Xu, Y. Hong, D. Bein, M. Levy, B. K. Sarma, S. Adenwalla, Z. Zhao, T. Tokuyasu, D. W. Hess, J. B. Ketterson, J. A. Sauls, and D. G. Hinks, Phys. Rev. Lett. **62**, 332 (1989).
[6]R. Joynt, Supercond. Sci. Tech. **1**, 210 (1988).
[7]R. A. Fisher, S. Kim, B. F. Woodfield, N. Phillips, L. Taillefer, K. Hasselbach, J. Flouquet, A. L. Giorgi, and J. L. Smith, Phys. Rev. Lett. **62**, 1411 (1989).
[8]K. Hasselbach, L. Taillefer, and J. Flouquet, Phys. Rev. Lett. **63**, 93 (1989).
[9]D. W. Hess, T. Tokuyasu, and J. A. Sauls, J. Phys. Cond. Matt. (to be published).
[10]K. Machida and M. Ozaki (unpublished).
[11]G. E. Volovik and L. P. Gor'kov, Zh. Eksp. Teor. Fiz. **88**, 1412 (1985) [Sov. Phys.—JETP **61**, 843 (1985)].
[12]P.W. Cooke *et al.*, Hyperfine Interact. **31**, 425 (1986).
[13]G. Aeppli, E. Bucher, C. Broholm, J. K. Kjems, J. Baumann, and J. Hufnagl, Phys. Rev. Lett. **60**, 615 (1988).
[14]M. Sigrist (private communication).
[15]W. O. Putikka and R. Joynt, Phys. Rev. B **37**, 2372 (1988).
[16]H. Monien and C. J. Pethick (unpublished).
[17]M. Norman, Phys. Rev. B **39**, 7305 (1989).
[18]G. Aeppli, D. Bishop, C. Broholm, E. Bucher, K. Siemensmeyer, M. Steiner, and N. Stüsser, Phys. Rev. Lett. **63**, 676 (1989).
[19]M. E. Zhitomirskii, Pis'ma Zh. Eksp. Teor. Fiz. **49**, 333 (1989) [JETP Lett. **49**, 379 (1989)].
[20]W. K. Kwok, L. E. DeLong, G. W. Crabtree, D. G. Hinks, and R. Joynt (unpublished).
[21]B. Shivaram, J. J. Gannon, and D. G. Hinks (unpublished).
[22]T. Tokuyasu, D. Hess, and J. Sauls (private communication).
[23]B. Shivaram, Y. H. Jeong, T. F. Rosenbaum, D. G. Hinks, and S. Schmitt-Rink, Phys. Rev. B **35**, 5372 (1987).